PCCP

Accepted Manuscript

This is an *Accepted Manuscript*, which has been through the Royal Society of Chemistry peer review process and has been accepted for publication.

Accepted Manuscripts are published online shortly after acceptance, before technical editing, formatting and proof reading. Using this free service, authors can make their results available to the community, in citable form, before we publish the edited article. We will replace this *Accepted Manuscript* with the edited and formatted *Advance Article* as soon as it is available.

You can find more information about *Accepted Manuscripts* in the Information for Authors.

Please note that technical editing may introduce minor changes to the text and/or graphics, which may alter content. The journal's standard Terms & Conditions and the Ethical guidelines still apply. In no event shall the Royal Society of Chemistry be held responsible for any errors or omissions in this *Accepted Manuscript* or any consequences arising from the use of any information it contains.

Butterfly effects: novel functional materials inspired from the wings scales

Wang Zhang, Jiajun Gu, Qinglei Liu, Huilan Su, Tongxiang Fan and Di Zhang*,

State Key Lab of Metal matrix Composites, Shanghai Jiaotong University, 800

Dongchuan Rd. Shanghai 200240 (P. R. China)

*zhangdi@sjtu.edu.cn

ABSTRACT Through millions of years of evolutionary selection, nature has created biological materials with various functional properties for survival. Many complex natural architectures, such as shells, bones and honeycombs, have been studied and imitated in the design and fabrication of materials with enhanced hardness and stiffness. Recently, more and more researchers have thrown themselves into the research on wings of butterflies because of their dazzling colors. It was found that most of these iridescent colors are caused by periodic photonic structures on the scales that make up the surfaces of these wings. These materials have recently become a focus of multidiscipline research because of their promising applications in the display of structural colors, advanced sensors, photonic crystals and solar cells. This review will provide a perspective overview of the research inspired from these wing structures in recent years.

KEYWORDS bioinspired, microstructures, optical, butterfly, wing scale

1. Introduction

Lepidoptera are a huge family with nearly 180,000 species [1], including butterflies and moths. These species (mostly are butterflies) have evolved many different kinds of wings to meet their survival or courtship needs [1]. Butterfly phylogeny has been shown to be related to the optical properties of these structures and to their evolutionary development [2]. More than twenty derived features can be used to characterize butterfly or moth species. One of the most apparent characteristics of these wings is the distinctive color of the scales that cover their wings and bodies. In butterfly wings, the colorization effects can involve pigment color and structural color and combinations of the two. The colors of butterfly scales are produced by pigments that selectively absorb lights with certain wavelengths. These pigments are embedded (some are called pigment beads, shown in Fig.1 S1) in the scale structures. These structures reflect and scatter light that has not been absorbed by the pigments [3]. However, structural color comes from the hierarchical structures in the wing scales. The brilliant colors generated at the sub-micrometer level by the complex architectures of the scales have attracted the interest of scientists from biology, physics, and materials science.[4]

In the last decades, many sagacious reviews and books have focused on the structural colors originated from butterfly wing scales. H. Ghiradella published the

first prospective overview and comprehensive classification of the development of the

precise and elaborate structures of butterfly wings, including hairs, bristles, and scales,

evaluating studies dating back to the 1970s [5]. Different research aspects of wing color

(especially the structural color), such as characterization, identification, and

mechanism were discussed by S. Berthier ten years ago [6]. An intensive study

classifying largely *Morphinae* and *Papilio* butterfly wing scales conducted by P.

Vukusic published later[7]. Research on optical properties and simulation fundamentals

of structural colors in *Lepidopter*a sub-families was summarized by S. Kinoshita in

chapter 3 of his book [8]. The tree-like structure in *Morphinae* wings, the most popular

butterfly which are very pleasing to the eye, have received much more attention

especially on their photonic properties [9]. A.R. Parker summarized the diversity and

evolution of the photonic structures in butterflies, including many of the early

unpublished works [10]. In summary, these overviews [5, 7, 8, 10-14] have supplied a

theoretical foundation for subsequent biomimetic fabrication.

Since the introduction of the concept of modern bio-mimetic materials in 1992

[15], many research groups have devoted their attention to the fabrication of

biomimetic materials inspired by natural microstructures. Several excellent reviews

and books on bioinspired and biomimetic materials have been published in the past

two decades [16-20]. In these studies, research into the biomimetics and biotemplates of

butterfly wings is considered ascendant due to the various complex and hierarchical

structures in these wings. Many novel applications related to the microstructures of

these bio-inspired materials have been explored. These include advanced structured colors[21], new generation solar cells[22], anti-counterfeiting labels[23], gas sensors[24], and high-speed infrared imaging [25]. Some of them have attracted considerable interest from government and industry [26]. The present work will present an overview of most recent developments in this blooming field. Since characterization and simulation of the butterfly wing scale microstructure have been summarized in the previous studies, the bio-mimetic and bio-template fabrication inspired by these wing scales have not been discussed thoroughly since the preliminary attempt by L.P. Biro [27]. Here, this review will present an intensive overview of research into the up-to-date fabrication methods of bioinspired artificial wing-like structures.

2. Brief introduction of the characterization and simulation of butterfly wing structures

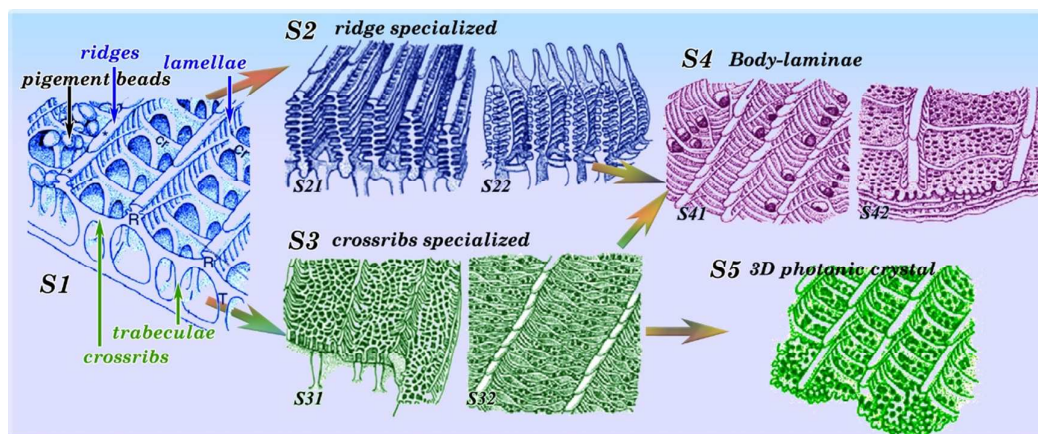### 2.1   Classification of butterfly wing structures

Butterflies may be the most conspicuous insects in the world, and has attracted a great deal of scientific and aesthetic interest. The butterfly individuals take advantage of these singularity optical effects to achieve different strategies, such as camouflage, courtship, communication, and sending warnings to predators [28-30]. Moreover, several studies have evaluated the enhancement effects of these microstructures on hydrophobicity and aerodynamic properties [31, 32].

The study of the relationship between color and the hierarchical microstructure in the butterfly wing scales has a long history, which is roughly simultaneous with the

development of the microscope. Ever since R. Hooke invented the optical microscope in 1665 [33], many pioneers have plunged into the studies on those colorful butterflies . Research took a leap before the development of the electron microscope, which established remarkably accurate physical structural models of butterfly wing [34, 35]. The most typical example is the characterization on the blue wings of *Morpho* butterfly. Early inquiries showed that the metallic blue color was attributable to a very thin surface layer and that the luster and brilliancy of the color were inconsistent with the thickness of the structure [34]. More than twenty years later, more careful characterization and preliminary simulation or modeling of the cause of the brilliant blue color of these scales was provided, although the modeling used in their work was later shown to be inaccurate [36]. Seventeen years later, microstructures, especially the cross-sections of the iridescent scales of *Urania* moths, were finally observed under electron microscopes and discussed in great detail [37]. Due to the continued improvement in the resolution of electron microscopes[38], much more complicated structures have been observed in each tiny scale of the butterfly wings. The research and understanding of butterfly wing structures has advanced from the micrometer to nanometer level.

Both structural colors and hydrophobic properties are derived from the cuticle structures of butterfly wing scales. In most species, the arrangement of the scales on the wing resembles that of shingles on a roof, each of the scales evolve from a single epidermal cell. A typical scale may be thought of as a flattened sac approximately

75 μm in width, 200 μm in length, and 5 μm in thickness. The walls of the sac become

the upper and lower surfaces, or laminae, of the scale. The lower surface, which faces

the membrane, is usually featureless, and the upper surface, which faces the outside,

has complicated shapes, such as gratings with longitudinal ridges joined at intervals

by cross-ribs. Different parts of the scales structure are labeled in Fig. 1 S1. These

structure groups are mainly based on the specialized regions in the scales, which are

shown in Fig. 1. S1 includes typical unspecialized wing scales. The upper surface of

these scales have longitudinal ridges roofed with overlapping lamellae. This covers a

series of folds (the microribs) that are perpendicular to the lamellae. The longitudinal

ridges are connected by crossribs. These form so-called windows to the interior of the

scale. The other four groups (S2-S5) of structures are arranged based on which

regions of the scale are modified. What is more, the relationship between the different

structures groups are marked on the scheme. The S2 type scales have highly

specialized ridges mainly developed from the upper structure (ridges and lamellae) of

scales. Through the evolution of the lower structure including crossribs and trabeculae,

the S3 type have porous windows between the ridges. Once both the upper and lower

structure are specialized, the S4 type will form body-laminae structure like multilayer

reflectors. The further crosslinking of the pores in S3, 3D photonic crystal structures

will developed in the scales. All the five structure groups and their characterization

are shown in Fig. 1 and listed in Table 1 (not an exhaustive list).

Figure 1. Five microstructure groups of butterfly wing scales. Ridges, crossribs (or horizontal struts), lamellae (or subribs), trabeculae (or vertical struts), and pigment beads are all marked in S1 [5].

2.2 Modeling and simulation of butterfly wing structures

In addition to the aerodynamic properties and surface hydrophobicity, the major focus of current research is the optical related properties of these wing microstructures. Many different mathematical algorithms have been developed and used to explain corresponding optical properties using Maxwell equations. Most of the size parameters of these microstructures can be measured carefully from traditional SEM, TEM, or advanced HIM images [38]. For the original butterfly wing scales, the most important parameter is the refractive index (RI) of chitin, the main component of the wings. Early in 1927, the RI was estimated to be about 1.55[35], which was closed to the recent data [39] (real component 1.56 ± 0.01 and imaginary component 0.06 ± 0.01) using index-matching techniques.

It is relatively difficult to find an index that precisely matches an immersion fluid. Several new experimental procedures were later developed. Using polarization reflectance spectra, the anisotropic refractive index of the chitin was investigated within a range of 350–800 nm [40]. The value (1.53–1.76) was shown to be consistent with those observed though the liquid index match technique in the 450–500 nm spectral range. Recently, the wavelength dependence of the refractive index of each immersion fluid was derived based on the Cauchy equation ($n(\lambda)=A+B/\lambda^2$) [41]. Based on these parameters, intensive studies were conducted on S2 [42] [43, 44] [45], S4[46, 47] [48] [23] and S5 [49] [50] type structures, which will guild the further fabrication and optimization design of novel functional materials inspired by butterfly wings.

3. *Progress in the fabrication of hierarchical functional materials inspired by* **butterfly** *wings*

The special functions of butterfly wings, especially in optics and hydrophobicity, has inspired material scientists constantly. Modeling and simulation results have improved the community's understanding of the subtle structures that guide the design and fabrication of advance functional materials. In this review, we will be more concerned on the recent progress in the fabrication of artificial functional materials both through direct templating using butterfly wings and through biomimetic approaches inspired by these wing scales. Table 1 summarizes the current state of the characterization, fabrication and applications novel materials inspired by different butterfly wing structure groups.

Table 1. Functional materials inspired by different butterfly wing structures

Wings scales		Characterization	Fabrication		Applications
Group	Subgroup		Biotemplating	Biomimetic	
I	S11	Unspecialized structure	Cathodoluminesnce and iridescence [51-54]	--	--
	S12	S11 studded with pigment beads	--	--	Enhancement of scattering; enhancement of white color
II	S21	Parallel ridges	Most studied group, especially for color display technology [21, 55-79]	Challenging to mimic the details of the structure. [80-84]	--
	S22	Inclined ridge-lamellae structures			Fabrication of biomimetic *morpho*-blue dye and fibers; highly selectivity and sensitive gas sensors
III	S31	Quasi-honeycomb structures	Light-harvesting properties. [22, 63, 71, 85-90]	Honeycomb structure by breath figure method. [91-94] [95-101]	Enhancement of the efficiency of light harvesting
IV	S41	Parallel laminae structures	Adjustment of color display by controlling the external field [102]	--	pH and micro-electricity sensors
	S42	Concave multi-layer structures	Templating method is difficult for the microstructure replication [76, 85, 86, 103, 104]	Combination of layer deposition techniques to mimic the color mixing effect [23, 105]	Anti-counterfeiting and colored paint
V	S5	3D photonic crystal microstructures	Successful fabrication of 3D photonic crystal (PC) gyroid structure [106, 107]	--	Fabrication of 3D photonic crystals with full band gap

3.1   Processes involved in fabrication methods that use butterfly wings as bio-templates

The wing scales are composed by trace proteins, pigments (mostly melanin), inorganic salts and chitin (more than 83%) [108]. Chitin, specifically α-chitin, is the

main component of butterfly wings, so most of the biotemplating processes are based on the chitin/chitosan chemistry[109]. It is made of units of N-acetylglucosamine and it forms covalent β-1,4 linkages similar to the linkages between the glucose units that form cellulose. In this way, chitin may be described as cellulose in which one hydroxyl group on each monomer has been replaced with an acetyl amine group. These free amino groups[78, 110] facilitate the biotemplating fabrication process. To expose more active reaction groups such as amino groups, deacetylation of the wing templates is very necessary before the templating process in alkaline environment, such as NaOH solution[111].

3.1.1 Sol-gel process

The *sol-gel* process is widely used in the fields of biotemplating and bioinspired fabrication. *Sols* are colloidal dispersions of particles in liquid. Colloids are solid particles with diameters of 1-100 nm. A *gel* is an interconnected, rigid network with pores of sub micrometer dimensions and polymeric chains whose average length is greater than a micrometer. The *sol-gel* processing is beneficial for the controlling the structure of material on nanometer scale from the earliest stage of processing [112]. Several different approaches have been developed to synthesize these ordered materials templated from natural materials based on *sol-gel* chemistry [113]. It is very suitable for the fabrication of the sorts of microstructures in butterfly wings because of its flexibility with respect to which chemicals are used, facile shape control, and mild reaction conditions.

In 2005, while searching for ways to fabricate three-dimensional photonic band gap (PBG) structures in large quantities Y_2O_3: Eu and TiO_2: Eu phosphor precursor solutions were used; air stable supersaturated europium-doped yttrium nitrate and air sensitive europium-doped titanium ethoxide respectively [64]. Negative replicas of the wings of *M. pleides* were successfully synthesized using this method. Though the filled-in samples (negative cast) did not show the photonic properties of the original butterfly scales, they did show that it was possible to reproduce fine details in these casts. The structural features of these replicas had dimensions of approximately 100 nm, but they also had cathodoluminescence properties different from those of nanocasts [114]. From the air stable supersaturated europium-doped yttrium nitrate solution previously developed for 3D PBG crystal template infilling [115] further wing scale casts were fabricated from *Sericinus montelus* specimens where FESEM studies confirmed nano-replication down to 20nm [116]. Because of the super-hydrophobic surfaces of most the butterfly wings [117], precursors with strong impregnation that could homogeneously soaked into wing templates are not easy to produce. The ethanol solutions of different metal nitrates were prepared and used to replicate butterfly wings with different microstructures [52-54]. The results showed that the fabrication of wings out of ZnO instead of chitin greatly enhanced the intensity of the optical reflectance of visible light, especially with the semi-transparent wing replicas based on the wings (S11) of *Ideopsis similis* [52]. Our later study evaluated the room temperature cathodoluminescence spectra of these ZnO replicas

templated from two wing scales with different structures (S31&S42) from *Papilio paris* forwings and hindwings [86]. Both spectra showed a similar sharp emission near the band-edge, but they showed different green emissions which may due to the different microstructures of the ZnO replicas. In addition to the mono component functional oxides, some complex composites and silicon carbide can also be obtained through the optimized *sol-gel* processes [103, 118, 119].

Later, a conformal and continuous nanocrystalline rutile TiO_2-based coating was generated on the *Morpho* butterfly wings using the computer controlled surface *sol–gel* coating process [118]. After 40 cycles of layer-by-layer deposition and subsequent 450°C firing, a replica showing the intricate and hierarchical 3D morphology of a *Morpho* wing including the nacrystalline rutile was produced and characterized. This process can also be expanded to other fabrication of nanocrystalline multicomponent oxides [62].
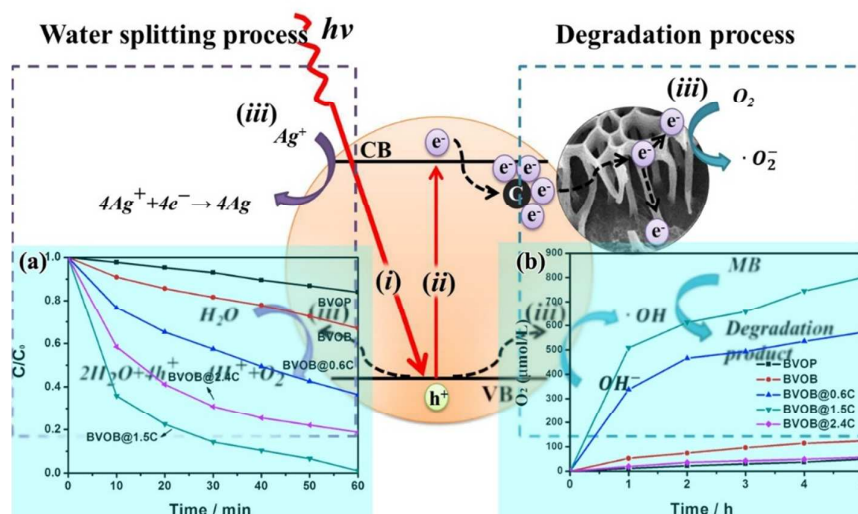
Figure 2. Background: The mechanism proposed for illustrating the role of hierarchical structures from butterfly wings and carbon in the photocatalytic performance of BVOB@1.5C (C-doped $BiVO_4$). (a) the photocatalytic degradation of MB at an initial concentration of 20 mg L^{-1} (50 mL) of BVOP and BVOB@xC under visible light irradiation ($\lambda > 420$ nm). The amount was kept the same for all the samples. The degree of MB photodegradation was obtained by calculating the change of concentration (C/C_0) from the variation of absorbance (A/A_0) at 665 nm, and (b) Photocatalytic O_2 evolution of the samples from aqueous $AgNO_3$ solutions (0.05 mol L^{-1}, 90 mL) under visible light irradiation ($\lambda > 420$ nm).[120]

Most of the works introduced above focused on fabrication technology, and increasing numbers of studies exploring new properties related to the specific hierarchical microstructures of the wings have been reported. Novel titania photoanodes with different butterfly wings for dye-sensitized solar cells were fabricated using modified titanium (IV) sulfide *sol-gel* as precursor [22]. Analysis of absorption spectra measurements in visible light indicated that photoanodes with quasi-honeycomb structures copied from *Paplio paris* black wing scales harvested light more efficiently than normal titania photoanodes due to the templated structure. This can increase the overall efficiency of solar cell systems and sunlight-based water-splitting catalysts [121, 122], and be benefit for the colloidal photonic crystals research [123]. The mechanism and the best photocatalytic activity in both photocatalytic

degradation and O_2 evolution from water splitting (ca. 800 μmol L^{-1}) was carefully

discussed and shown in Fig. 2.[120]

Besides the ethanol solutions, it is also possible to use an aqueous *sol–gel* process to

replicate butterfly wings by pretreating original wing templates with ethanol. With the

help of ethanol pre-treatment, it is possible to use an aqueous *sol–gel* process to

replicate butterfly wings. This process was later developed into an aqueous *sol-gel*

process assisted by ethanol-wetting to minimize the surface hydrophobicity [65, 66, 124].

The SnO_2 replicas of *Euploea mulciber*, which had coatings of different thicknesses,

showed controllable sensitivity to ethanol and formaldehyde. This demonstrated that

such structures could not only enhance the gas response but also provide good

selectivity. It was also found that the gas response could be significantly affected by

membranous structures. This mechanism was different from the optical gas sensitive

response of the original *Morpho* butterfly wings[24], which showed a high selectivity

vapor response [24, 122]. The linear relationship between the effective refractive index

and the liquid quantity was later observed and simulated later [125].

Optical properties especially the selective or angle depend reflective properties is

the major research interest in the bio-template materials research. Enhanced or

modified optical properties of the original wings were studied. In earlier work, the

whole wings were used as the biotemplates, so large-area (about 3×4 cm^2) optical

inorganic wings were synthesized [52, 67, 126]. These replicas can reflect visible or

ultraviolet light strongly because of the relatively large refractive index of functional

oxides. Other oxides, such as ZnO, SnO$_2$, and SiO$_2$ *etc.* were also fabricated using the

sol-gel process with ultrasonication [56, 87]. Different reflective spectra of these replicas

showed the pronounced influence of the effective refractive index on the optical

properties.
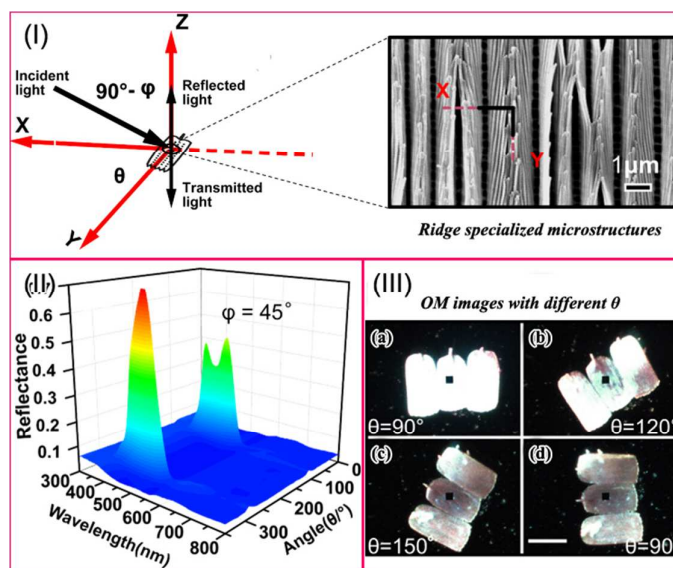
Figure 3. Schematic illustration of reflectance measurement setup and

corresponding spectrum results. (I) Angle dependent reflectance measurement setup

in this work. The SEM image was taken from an original butterfly wing scale. (II)

Angle dependent reflectance spectra ($\varphi = 45°$, θ moves from 0° to 360°). (III) Optical

microscope images of measured SWSs with different θ. Scale bar = 100 μm.[57]

To distinguish single scale and scales arrangement influence on the optical

performance, one study evaluated isolated scales using different scales with static

needles early in 1999 [39]. Single scales with different types were selected as templates

[57, 68]. Spatial optical anisotropy of ZnO (shown in Fig. 3) and ZrO$_2$ were templated

from isolated scales of *M. menelaus* and *M. didius*. Because there can be as many as

600 individual scales *per* square millimeter of wing surface, this work presents a potential route for large-scale production of small, complex photonic devices using these wing scales as building blocks. This approach may also offer many different model systems for 3D photonic crystal (PC) research [69]. As the strength of external magnetic field increased, the reflectance spectra of the Fe_3O_4 replica of the wings was red-shifted. This type of tunability opens up an avenue for the creation of new magneto-optical devices and may inspire theoretical studies in the field [70]. Inorganic (SiO_2 and TiO_2) chiral 3-D PC with bicontinuous gyroid structure (S5) were replicated from *C. rubi* wing scales using a similar *sol-gel* process [106, 107] (shown in Fig. 4). The replica has an equivalent unit cell, an increased fill fraction and decreased dielectric constant relative to its chitin template. Thus the change in the dielectric contrast is the main factor for the observed blue shift upon replication. The 3D SiO_2 and TiO_2 photonic crystals replicated in C. Mille's work have nearly complete overlapping of partial band gaps, strongly suggesting that materials with full photonic band gaps are experimentally within reach.
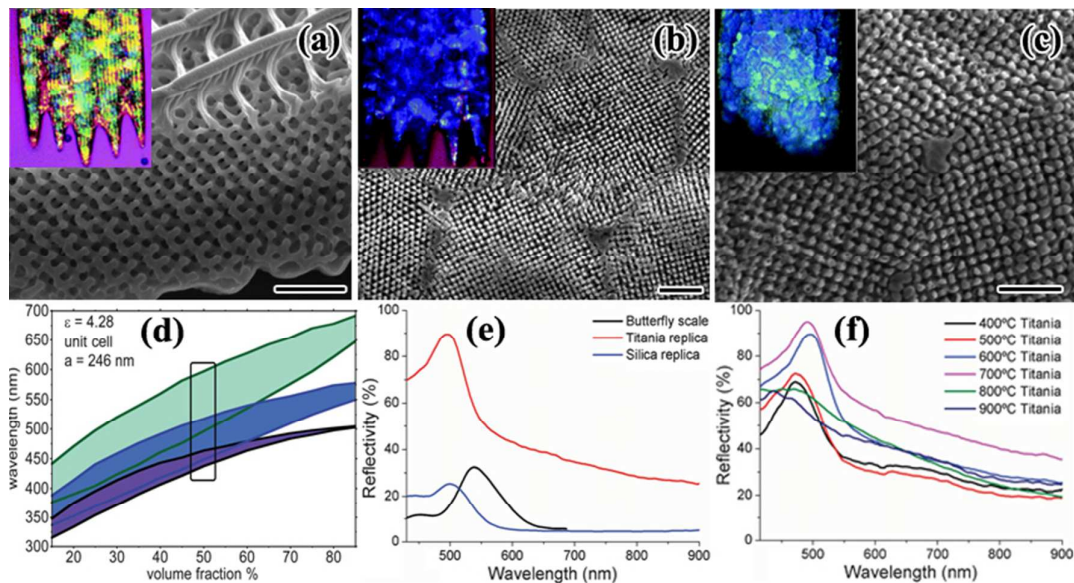
Figure 4. SEM images of cross-section of original *C. rubi* wing scales (a) and SiO₂ (b), TiO₂ (c) scale templated from (a). Insets of (a), (b), (c) represent the optical image of relative scales. Scale bars are all 1μm for (a), (b) and (c). (d) is the partial band gap map for titania as a function of solid volume fraction featuring the partial band gaps, shown as colored regions. Note the shift to lower wavelengths with decreasing volume fraction. The region denoted by the rectangle centered near 50% volume fraction is a zone of reasonable fit to the observed spectral data. The three primary bands correspond to the Γ–N, Γ–P and Γ–H directions, *i.e.*, the ,<110>, <111> and<100>. Crystallographic directions, represented in light green, blue, and purple, respectively. (e) Representative reflectivity spectra of *C. rubi* and silica and titania replicas with the position of the reflection maxima centered at 540 nm, 500 nm, and 505 nm, respectively. Note that the maximum reflectivity of silica (y25%) is below that of the original butterfly scale. The titania replica shows a reflectivity maximum of

90%. (f) Comparison of the spectra obtained from titania photonic crystals calcined between 400 °C and 900 °C.[106, 107]

Metals, including Co, Ni, Cu, Pd, Ag, Pt, and Au, which are shown in Fig. 5 II, can also be reduced using the electroless deposition methods in the *sol-gel* solution [77, 78]. The Au, Ag, and Cu replicas of butterfly wing scales were found to have markedly more pronounced Raman scattering (SERS) effects than replicas made of other materials. The pronounced Raman enhancement mainly originates from the 3D sub-micrometer periodic rib-structures located on the main ridges of Cu scales rather than the morphological or size effects of Cu NPs themselves[79]. Similar to the more floors a building has, the more residents it can contain, more periodically arranged rib-layers *per* unit square result in more piled-up hotspots, leading to better SERS performance. This is because of the accumulation of hotspots, which are located at sites where the local electromagnetic fields are markedly enhanced. These hotspots are produced by the intrinsic 3D sub-micrometer structures of the metals. SERS has attracted a great deal of attention due to its ability to facilitate fast detection of trace amounts of chemicals. Metallic SERS substrates can enhance the weak Raman signals of analytes adsorbed on them by several orders of magnitude. However, the low reproducibility and high cost of SERS substrates as consumables restrict their use. In comparison, the sensitivity of the system's ability to detect Rhodamine 6G (R6G) on Au (10^{-13} M) is ten times higher than that of its ability to detect R6G on Klarite® (10^{-12} M), which is the commercial SERS substrate. Considering the high cost and the

sensitivity of detection on metallic butterfly wings, this strategy may render affordable and stable SERS substrates accessible to laboratories across the world. By combining well-developed tuning methods with these natural designed 3D scaffolds, the morphology of the nanometal particles and the formation of structures with multiple components can be controlled [127]. Even higher SERS performance can be expected.
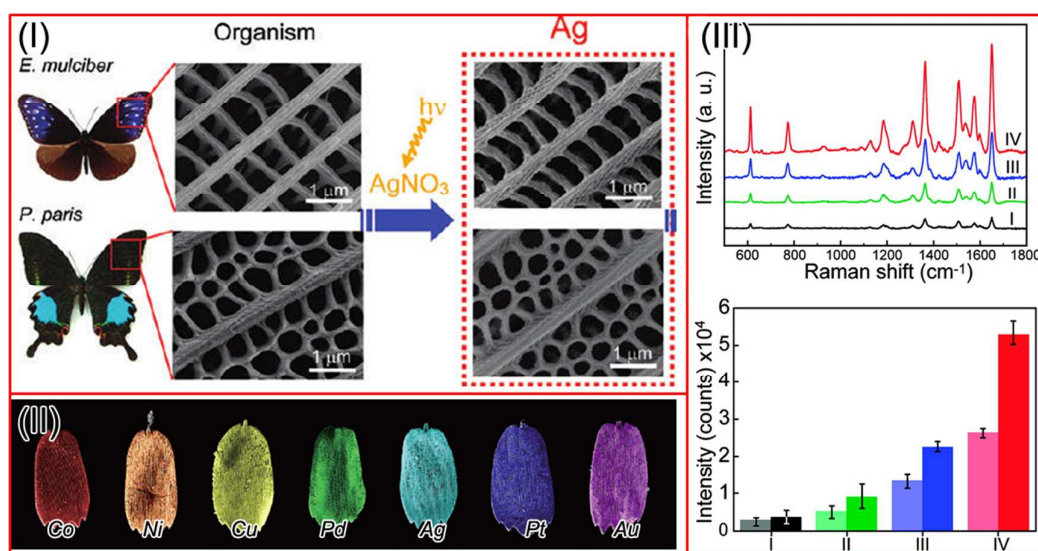
Figure 5. (I) Fabrication of Ag-replicas of butterfly wings [77]. (II) Pseudo-color SEM images of seven metallic wing-scale replicas [78]. (III) (a) SERS spectra of a 10^{-3} M R6G solution on substrate I (a smooth, thin Ag film), substrate II (Ag nanoparticles ground from the biotemplated Ag replicas using an agate mortar), substrate III (Ag replica with the quasi-periodic submicrostructures prepared using *P. paris* as a template, and substrate IV (Ag replica with the periodic submicrostructures replicated from *E. mulciber*). (b) Comparison of the 612 cm^{-1} (left column) and 1364 cm^{-1}(right column) SERS signal band areas of R6G for the four types of substrates in (a). The

intensities of the R6G Raman signals on substrate IV were approximately 15, 6, and 2 times higher than those of substrates I–III, respectively [77].

3.1.2 Nanoimprintating process

Nanoimprint lithography (NIL) shows considerable promise due to its low cost, high throughput capacity, and ability to imprint large areas. It creates patterns using mechanical deformation of imprint resist and subsequent processes[128]. The imprint resist is typically a monomer or polymer formulation that is cured by heat or UV light during the imprinting. Adhesion between the resist and the template is controlled to allow proper demoulding. This procedure usually requires the fabrication of master-molds by conventional microelectronics techniques, such as lithography and etching. These are time-consuming and limited in scale. The preparation of stamps that maintain high resolution over large areas is key to NIL. Many efforts have been made to develop stamps with different alignment structures, especially bionanostructures, such as those of leaves and insect wings, to resolve the problem of micro- and nanostructure imprinting[129, 130]. Using these techniques, some research groups have used natural butterfly wings as master-molds to cast elastomeric templates, both negative and positive structures of the original wings. This simplified the fabrication process and allowed the reproduction of the original complex patterns on the wings.

The wing of *P. ulysses* has concavity microstructures and multilayers of about five to ten periods. This wing was chosen for replication using flexible

polydimethylsiloxane (PDMS) [104]. Because of the low Young modulus of the PDMS (around 0.8 MPa), the as-synthesized templates can replicate the concave curvature of the surfaces of the butterfly wings. This makes them suitable for use in imprint spin-coated resistant films at low pressures. Methyltriethoxysilane (MTEOS) *sol-gel* films were prepared for the imprint at a pressure of under 2 bars. The temperature was kept between 80°C and 150°C and the process lasted about 20 min. This technique produces a multilayered structure, and it is well suited to producing the tree-like structures of *Morpho* wings. The results of absorptivity, reflectivity, and fluorescent characteristics of the replicas showed that the microstructural and optical characteristics of the replicated wing were qualitatively consistent with those of actual wings [82]. Researchers believed that this technique may represent a viable approach to the mass production of artificial PC structures suitable for a variety of commercial applications. First, electric field and pH sensors were produced by filling the multilayer structures (*C. rhipheus*, S4) with electric-field-sensitive or pH-sensitive hydrogels [102] [131]. The visible reflectance of the immobilized wing scales was found to be responsive to electric field and pH conditions (shown in Fig. 6). This was attributable to the inner microstructural changes induced by the changes in the volume of the embedded polymer during the swelling/deswelling process. The pH-induced color change was detected by reflectance spectra as well as optical observation. A distinct U transition with pH was observed, demonstrating PMAA content-dependent properties. These work sets up a strategy for the design and fabrication of tunable

photonic crystals with hierarchical structures, which provides a route for combining

functional polymers with biotemplates for wide potential use in many fields.[110, 131].
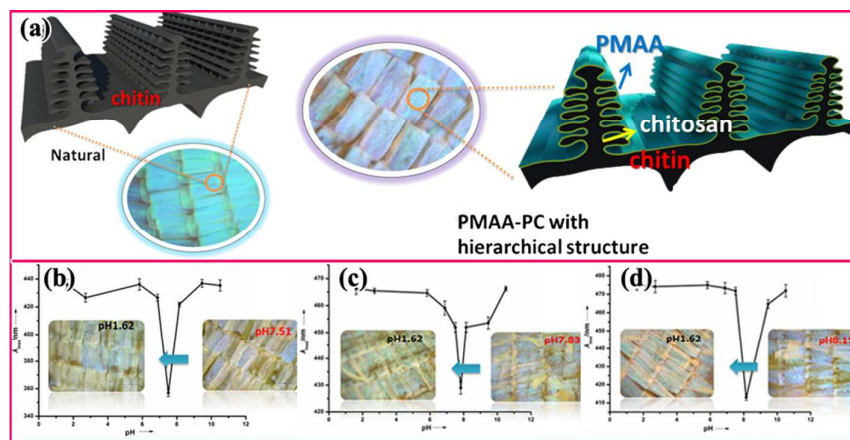
Figure 6. The upper column: (a) Overall synthesis of pH-responsive PCs from

Morpho butterfly wings. Lower column: Representative spectral responses of (b)

PMAA-PC-1, (c) PMAA-PC-2, and (d) PMAA-PC-3 to different pH values, with

representative optical images obtained at typical pH values.[110]

3.1.3 Vapor phase deposition

Vapor phase deposition is a process in which gas phase transforms into solid phase.

It is wildly used in thin-film coating. Two major vapor phase deposition techniques,

chemical vapor deposition (CVD) and atomic layer deposition (ALD), are based on

the sequential use of a gas phase chemical process. ALD is chemically similar to

CVD, except that the ALD reaction breaks the CVD reaction into two half-reactions,

keeping the precursor materials separated during the reaction. Because its reactions

are self-limiting and take place on the surface of the substrate, ALD makes atomic

scale deposition control possible [132, 133]. Compared to CVD, ALD can provide a

simple and accurate thickness control as it can be controlled with every cycle. Furthermore, ALD offers facile doping, large area uniformity and thus straightforward scale-up [133]. The advantage is obvious, as this method can be applied to most materials which can be deposited by ALD, especially on the soft and fragile butterfly wing templates [21].

Early in 2003, the technique involving controlled vapor-phase oxidation of silanes on the surface of peacock butterfly wings was used to produce exact inorganic oxide replicas of structures observed in nature [51]. The primary silica clusters had extraordinary flow properties and were found capable of creeping into smallest gaps within the wings. In this way, this method shows promise for the replication of these intricate hierarchical structures. However, the incompatibility between butterfly wings and the silane coating can cause catastrophic cracking of the coating during calcination, as observed under SEM.

To fabricate high-fidelity replicas of different biotemplates, another film deposition process, conformal evaporated film by rotation (CEFR), was developed[89, 90]. The CEFR technique is particularly well suited to biomimetization because the temperatures involved are sufficiently low and the replication process occurs in a noncorrosive environment, which prevents damage and distortion of the C-, H-, and O-based organic skeletons. By controlling the current and vapor flux, a $0.5\ \mu m$ coating was placed on the wings. Because the morphology of the butterfly wing makes it a very efficient diffuser of light, the chalcogenide glass ($Ge_{28}Sb_{12}Se_{60}$)

replica of *Battus philenor*, which has a large index of refraction within the visible and infrared spectra, could be used as an antireflection structure for increased photon trapping and optical diffusers.

The thickness of the coating was not very easy to adjust through the amount of silane precursor and the reaction time of CVD technique or current and flux of CEFR. In order to overcome these problems, the atomic layer deposition (ALD) technique was used in the replication of butterfly wings [21]. ALD is a self-limiting, sequential surface chemical technique that deposits thin, conformal films of materials onto substrates of varying compositions[134]. This mechanism facilitates the growth of conformal thin films of specific thicknesses on large areas. By keeping the precursors separate throughout the coating process, control of the growth of atomic films can be rendered as fine as ≈ 0.1 Å (100 pm) per cycle. These advantages make the ALD method suitable for the more exact replication of natural materials with 3D hierarchical structures. Z.L. Wang's *et al.* were first to use the atomic layer deposition approach to replicate and coat the photonic structures of *M. peleides*[21]. The growth rate was 1 Å per cycle, which allowed exact control of the thickness of alumina replicas of the wings (Fig. 7(a)). The alumina replicas also exhibited optical properties that facilitated applications in waveguides and beam splitters. Further research into the influence of layer thickness on the optical properties was performed using ALD on the iridescent green scales (S42) of *P. blumei* [135]. Studies have shown that, depending on the structural integrity of the initially sealed scale, it is found possible to

replicate not only the outer but also the inner surfaces of the structure, which may be more complex than the outer surfaces. Each of these replication processes produces distinct multicolor optical properties, as shown by experimental and theoretical data. One recent study evaluated the influence of layer thickness on the reflectance properties and the corresponding angle-resolved optical performance of alumina wing replicas using the higher aspect ratio microstructure of *M. menelaus* [55]. The ALD replication process makes it possible to use these precise replicas as building blocks for photonic integrated circuit systems with higher reproducibility and lower fabrication costs than traditional lithography techniques. Results showed that the optical properties could be adjusted with layer thickness. The surface properties of the wings were also studied [136]. However, these results were not consistent with measured values. The surface coating (30 nm) on *M. peleides* was found to change the surface from hydrophobic to hydrophilic [136]. Recent research on thinner coatings (20 nm) of *M. menelaus* showed that both coated and uncoated surfaces were hydrophobic[55].
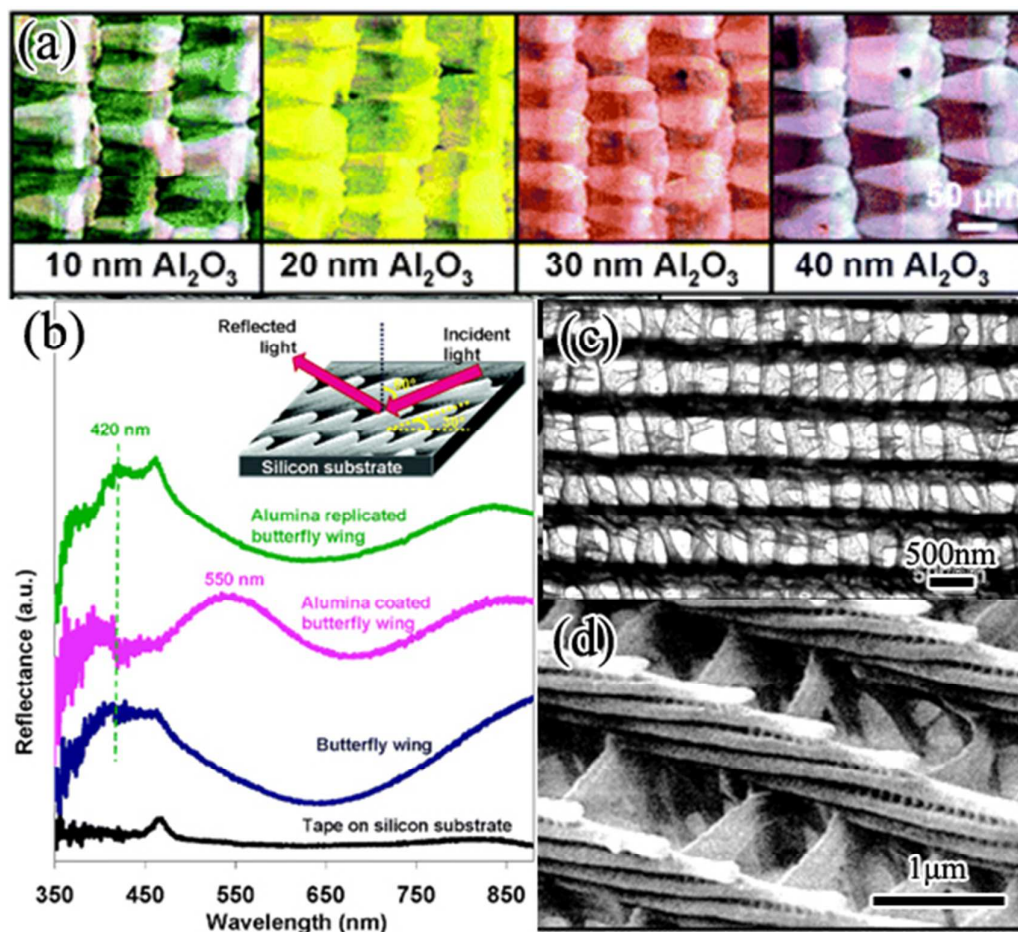
Figure 7. Images and optical spectra of the alumina replicas of the butterfly wing scales. (a) Optical microscope images of alumina-coated butterfly wing scales, whose color changed from original blue to pink. (b) Reflectance spectra of the original butterfly wings, alumina-coated wings, alumina replicas, and carbon tape background in UV-visible light range. The inset is the schematic of reflection measurement setup. (c) Low-magnification TEM image corresponding to the typical structure of an alumina replicated scale. (d) Higher magnification SEM image of an alumina replicated scale, which shows that the replica had exactly the same fine structures. [21]

3.2 Biomimetic processing methods used to produced materials inspired by butterfly wings

This review concentrates on two radically different ways of using the highly sophisticated structures that butterfly wing microstructure have developed. The first one consists of copying or templating the structure, for example using chemical or thermal transformation of the natural material (the above section). The second one strives at extracting materials concepts and implementing them in the fabrication of engineering materials (this section) [137]. In particular, biomimetic research is a much longer process involving an in-depth study of the microstructure characterizations of the scale's microstructure. Several biomimetic fabrication processes were developed to address the limitations of direct templating methods, such as template selection, uniform batch production, and large-scale use.

The very first material fabrication inspired by butterfly wing microstructure was proposed by Shimoyama *et al.* [138]. This team developed tunable structural-color devices using an electrostatic comb-drive actuator. An interference film was formed by deposition of a thin layer of parylene onto the comb-drive actuator. This actuator was made through conventional semiconductor fabrication techniques. Late the blue color similar to *Morpho* wing using TiO_2/SiO_2 multi-layers deposited on the stepped quartz was reproduced by electron beam lithography and dry etching [74]. Though the simplified design of the discrete multilayer film was quasi one-dimensional pattern, the results showed that the optical scattering property was dominated by structures on

the 100–300 nanometer scales. Two years later, a new process was used to reproduce the *Morpho* blue color, which was generated by the combination of nanocasting lithography (NCL) and electron beam deposition to create an analogue of butterfly nanostructures [72, 73]. Using the modern focused ion beam chemical vapor deposition (FIB-CVD), the same shape and size as the original *Morpho* blue wing scales were fabricated [80, 81]. Although it has shown promise in replicating the wing nanostructures with useful optical properties, the FIB-CVD approach also has several drawbacks. It lacks scalability and is not cost-effective. Then, nano-imprint lithography (NIL) and shear patterning techniques were combined to emulate the elaborate architecture of the butterfly wings conveniently [83]. They, however, did not attempt to control the color of the synthetic wing structures, which may be possible through tuning of the geometry, shape, and material of the nanostructures.
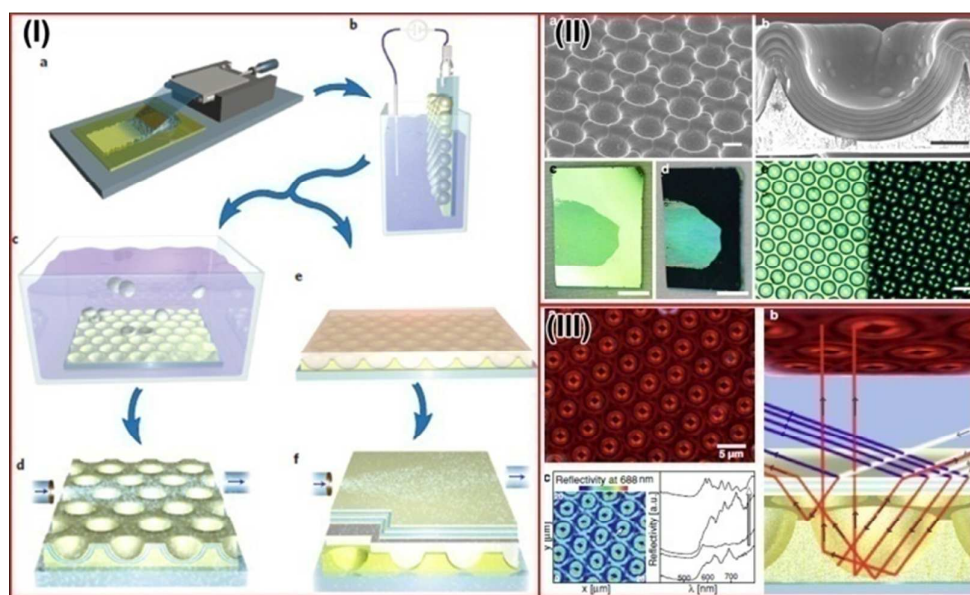
Figure 8. (I) Sample fabrication. (a) Deposition of polystyrene colloids on a gold-coated silicon substrate. (b) Growth of platinum or gold in the interstices of the colloidal array via electro-plating. The metal deposition is terminated when the thickness of the deposited film equals the microsphere radius. (c) Removal of the polystyrene spheres from the substrate by ultra-sonication in acetone. (d) Sputtering of a thin carbon film and atomic layer deposition of a stack of 11 alternating TiO_2 and Al_2O_3 layers (arrows indicate the precursor gas flow). (e) In a second route, the colloids are melted and cover the cavities with a homogeneous film. (f) TiO_2 and Al_2O_3 multilayers are deposited onto this film [23] (II) An artificial optical mimic. SEM images show concavities covered by a conformal multilayer stack of 11 alternating layers of TiO_2 and Al_2O_3: (a) *top view*, 2 μm, (b) cross-section, 1 μm. (c) At perpendicular light incidence the artificial replica appears green. (d) It reflects blue at grazing incidence, showing some iridescence, *scale bars* 5 mm. (e) Under a light microscope, the concavity edges appear turquoise, and the centers and interstitial regions appear yellow, scale bar 5 nm. (III) The modified mimic in the dark field. (a) Dark field micrograph. (b) Illustration of different light paths in the cavity. (c) Intensity map of some cavities at λ= 688 nm (left) and reflection spectra (right) acquired along the white arrow shown in the intensity map [105].

Some hybrid processes have been developed to produce materials that mimic the wings' microstructures more faithfully than previous research the last two years. In 2010, M. Kolle *et al.* combined colloidal self-assembly, sputtering, and ALD in the

fabrication a novel photonic structures that mimic the blue scales of *Papilio blumei* [23]. The details of the process are shown in Figure 8. They demonstrated that small variations in the natural design principle could allow a striking color separation effect. These square-centimeter-sized patterns and pictures, which had microscale resolution, were encoded in the photonic structure. This made this approach very versatile and suitable for applications in security labeling. This may benefit the future anti-counterfeiting efforts. M. Crne *et al.* later described the results of mimicking the *Papilio palinurus* structure through deposition of multilayers of titania and alumina using ALD over a polymer film with an ordered array of monodisperse micron size pores formed using breath figure (BF) process[139, 140].

Many successfully methods for constructing ordered honeycomb structures have been developed in large scale. However, these top-down methods usually involve complicated and expensive facilities, such as FIB, e-beam lithography *etc*. Since the introduction of the BF fabrication method by Francois *et al* [141], honeycomb films constructed by the BF method have been paid a lot of attention. Several research groups, such as M. Shimomura[91, 92, 142-144], L. Billon[95, 97, 99, 101], A. Bolognesi & F. Galeotti[96, 98], have performed systematic work. In this method, water droplets condense on the cooled surface of a polymer solution as a result of evaporative cooling, and are subsequently packed by capillary forces. After evaporation of the solvent, traces of the water droplets remain in the polymer film as a regular array of micropores. Nearly all kinds of building units could be involved in the process, such

as starlike polymers[145], block copolymers[146], organic-inorganic hybrids[147], ligand-stabilized metal nanoparticles (NPs)[148, 149], and surfactant-encapsulated polyoxometalates[150]. Various applications could be applied, especially in separation membranes[151], super-hydrophobic materials [94], photonic or optoelectronic devices [152], cell-culturing substrates [153, 154], and micropatterning templates [155-157].

4. Conclusion and future outlook

Attracted by the fascinating subtle structures of butterfly wing scales, more and more interest has been gained during the past decade. For the re-production of these structures in lab, one still misses an exact and convenient technique that would allow an excellent replication of the original wing scales microstructures. Biotemplating makes it possible, even easy, to maintain the complexity of the original structures, but it is not suitable for batch fabrications. Biomimetic methods can be used to produce uniform materials but they cannot readily be used to mimic the original hierarchical microstructures of the butterfly wings. Herein, through the comparison and evaluation of various methods for preparing, a potential method combined both biotemplating and biomimetic concepts have been developed. In this process, the Fe@Carbon replicas of wing scales was used as second imprinting template, massive biomimetic butterfly wing scales structures could be reproduced.[158] That is the first step to combine both the benefits of biotemplating and biomimetic, though the second imprinting microstructure is not as perfect as the original scale. Also, more simulations and design research must be performed before biomimetic fabrication can

become a reality on any practical scale. The optimization of proper structures and

extraction of the key parameters with corresponding properties may guide and

simplify synthesis of materials.[45, 159] The ultimate aim of the current work is to design

and optimize various functional materials based on the different structures effected by

the butterfly wings.

5. *Acknowledgement*

1.   R. G. Foottit and P. H. Adler, *Insect biodiversity: science and society*,
        Blackwell Pub2009.
2.   S. Wickham, M. Large, L. Poladian and L. Jermiin, *J. R. Soc. Interface*, 2006,
        3, 99.
3.   D. G. Stavenga, M. A. Giraldo and H. L. Leertouwer, *J. Exp. Biol.* , 2010, **213**,
        1731-1739.
4.   S. Berthier, *Iridescences: the physical colors of insects*, Springer, New York,
        NY, 2007.
5.   H. Ghiradella, *Microscopic anatomy of invertebrates*, 1998, **11**, 257-287.
6.   S. Berthier, *La couleur des papillons ou l'impérative beauté: propriétés
        optiques des ailes de papillons*, Springer2000.
7.   P. Vukusic and R. Sambles, *Physics, Theory, and Applications of Periodic
        Structures in Optics*, 2001, **4438**, 85-95.
8.   S. Kinoshita, *Structural colors in the realm of nature*, World Scientific Pub Co
        Inc2008.
9.   S. Berthier, *Photonique des Morphos*, Springer2010.
10.   A. L. Ingram and A. R. Parker, *Philosophical Transactions of the Royal
        Society B-Biological Sciences*, 2008, **363**, 2465-2480.

11. H. Ghiradella and W. Radigan, *J. Morphol.* , 1976, **150**, 279-297.

12. H. Ghiradella, *Insect cuticular surface modifications: scales and other structural formations*2010.

13. P. Vukusic, *Functional Surfaces in Biology*, 2009, 237-258.

14. S. Kinoshita and S. Yoshioka, *Chemphyschem*, 2005, **6**, 1442-1459.

15. A. Heuer, D. Fink, V. Laraia, J. Arias, P. Calvert, K. Kendall, G. Messing, J. Blackwell, P. Rieke and D. Thompson, *Science*, 1992, **255**, 1098.

16. S. Sotiropoulou, Y. Sierra-Sastre, S. Mark and C. Batt, *Chem. Mater.* , 2008, **20**, 821-834.

17. K. Liu and L. Jiang, *ACS nano*, 2011, **5**, 6786-6790.

18. M. H. Bartl, J. W. Galusha and M. R. Jorgensen, eds. J. Wu, J. Cao, W.-Q. Han, A. Janotti and H.-C. Kim, Springer New York2012, vol. 149, pp. 175-207.

19. Y. Liu, J. Goebl and Y. Yin, *Chem. Soc. Rev.* , 2013.

20. F. P. Barrows and M. H. Bartl, 2014.

21. J. Huang, X. Wang and Z. Wang, *Nano Lett.* , 2006, **6**, 2325-2331.

22. W. Zhang, D. Zhang, T. Fan, J. Gu, J. Ding, H. Wang, Q. Guo and H. Ogawa, *Chem. Mater.* , 2009, **21**, 33-40.

23. M. Kolle, P. M. Salgard-Cunha, M. R. J. Scherer, F. Huang, P. Vukusic, S. Mahajan, J. J. Baumberg and U. Steiner, *Nat Nano*, 2010, **5**, 511-515.

24. R. A. Potyrailo, H. Ghiradella, A. Vertiatchikh, K. Dovidenko, J. R. Cournoyer and E. Olson, *Nat. Photonics* 2007, **1**, 123-128.

25. A. D. Pris, Y. Utturkar, C. Surman, W. G. Morris, A. Vert, S. Zalyubovskiy, T. Deng, H. T. Ghiradella and R. A. Potyrailo, *Nat Photon*, 2012, **6**, 195-200.

26. Butterfly tech team: DARPA nod 'detonates' status quo, http://www.gereports.com/butterfly-tech-team-darpa-nod-detonates-status-quo/.

27. L. P. Biro and J. P. Vigneron, *Laser & Photonics Reviews*, 2011, **5**, 27-51.

28. A. Sweeney, C. Jiggins and S. Johnsen, *Nature*, 2003, **423**, 31-32.

29. S. M. Doucet and M. G. Meadows, *J. R. Soc. Interface*, 2009, **6**, S115-S132.

30. D. J. Kemp, *P Roy Soc B-Biol Sci*, 2007, **274**, 1043-1047.

31. N. D. Wanasekara and V. B. Chalivendra, *Soft Matter*, 2011, **7**, 373-379.

32. Y. Fang, G. Sun, Q. Cong, G. H. Chen and L. Q. Ren, *J. Bionic Eng.* , 2008, **5**, 127-133.

33. R. Hooke, *Micrographia: or some physiological descriptions of minute bodies, made by magnifying glasses with observations and inquiries thereupon*, James Allestry1665.

34. C. W. Mason, *J Phy. Chem.*, 1926, **30**, 383-395.

35. C. W. Mason, *J Phy. Chem.*, 1927, **31**, 321-354.

36. T. F. Anderson and A. G. Richards, *J. Appl. Phys.* , 1942, **13**, 748-758.

37. W. Lippert and K. Gentil, *Zoomorphology*, 1959, **48**, 115-122.

38. S. A. Boden, A. Asadollahbaik, H. N. Rutt and D. M. Bagnall, *Scanning*, 2011, n/a-n/a.

39. P. Vukusic, J. R. Sambles, C. R. Lawrence and R. J. Wootton, *P Roy Soc B-Biol Sci*, 1999, **266**, 1403-1411.

40. S. Berthier, E. Charron and A. D. Silva, *Optics Communications*, 2003, **228**, 349-356.

41. H. L. Leertouwer, B. D. Wilts and D. G. Stavenga, *Opt. Express* 2011, **19**, 24061-24066.

42. A. Mejdoubi, C. Andraud, S. Berthier, J. Lafait, J. Boulenguez and E. Richalot, *Physical Review E*, 2013, **87**, 022705.

43. R. Lee, Doctor, Georgia Institute of Technology, 2009.

44. R. Lee and G. Smith, *Appl. Opt.* , 2009, **48**, 4177-4190.

45. W. Wang, W. Zhang, W. Chen, J. Gu, Q. Liu, T. Deng and D. Zhang, *Opt. Lett.* , 2013, **38**, 169-171.

46. P. Vukusic, J. Sambles and C. Lawrence, *Nature*, 2000, **404**, 457.

47. P. Vukusic, R. Sambles, C. Lawrence and G. Wakely, *Appl. Opt.* , 2001, **40**, 1116-1125.

48. J. P. Vigneron, M. Ouedraogo, J. F. Colomer and M. Rassart, *Physical Review E*, 2009, **79**.

49. M. Saba, M. Thiel, M. D. Turner, S. T. Hyde, M. Gu, K. Grosse-Brauckmann, D. N. Neshev, K. Mecke and G. E. Schroder-Turk, *Physical Review Letters*, 2011, **106**, 103902.

50. B. D. Wilts, K. Michielsen, H. De Raedt and D. G. Stavenga, *Interface Focus*, 2011.

51. G. Cook, P. Timms and C. G ltner-Spickermann, *Angew. Chem. Int. Ed.* , 2003, **42**, 557-559.

52. W. Zhang, D. Zhang, T. X. Fan, J. Ding, J. J. Gu, Q. X. Guo and H. Ogawa, *Bioinspir. Biomim.*, 2006, **1**, 89-95.

53. W. Zhang, D. Zhang, T. X. Fan, J. Ding, Q. X. Gu and H. Ogawa, *Nanotechnology*, 2006, **17**, 840-844.

54. W. Zhang, D. Zhang, T. X. Fan, J. Ding, Q. X. Guo and H. Ogawa, *Microporous and Mesoporous Materials*, 2006, **92**, 227-233.

55. F. Liu, Y. P. Liu, L. Huang, X. H. Hu, B. Q. Dong, W. Z. Shi, Y. Q. Xie and X. A. Ye, *Optics Communications*, 2011, **284**, 2376-2381.

56. S. Zhu, D. Zhang, Z. Chen, J. Gu, W. Li, H. Jiang and G. Zhou, *Nanotechnology*, 2009, **20**, 315303.

57. Y. Chen, X. N. Zang, J. J. Gu, S. M. Zhu, H. L. Su, D. Zhang, X. B. Hu, Q. L. Liu, W. Zhang and D. X. Liu, *J. Mater. Chem.* , 2011, **21**, 6140-6143.

58. M. R. Weatherspoon, Y. Cai, M. Crne, M. Srinivasarao and K. H. Sandhage, *Angew Chem Int Edit*, 2008, **47**, 7921-7923.

59. X. Y. Liu, S. M. Zhu, D. Zhang and Z. X. Chen, *Mater Lett*, 2010, **64**, 2745-2747.

60.   O. Sato, S. Kubo and Z. Z. Gu, *Accounts Chem Res*, 2009, **42**, 1-10.

61.   W. Zhang, D. Zhang, T. Fan, J. Ding, Q. Guo and H. Ogawa, *Nanotechnology*, 2006, **17**, 840-844.

62.   J. P. Vernon, Y. N. Fang, Y. Cai and K. H. Sandhage, *Angew. Chem. Int. Edit*, 2010, **49**, 7765-7768.

63.   H. H. Liu, QibinZhao, H. Zhou, J. Ding, D. Zhang, H. X. Zhu and T. X. Fan, *Phys Chem Chem Phys*, 2011, **13**, 10872-10876.

64.   J. Silver, R. Withnall, T. G. Ireland and G. R. Fern, *Journal of Modern Optics*, 2005, **52**, 999-1007.

65.   F. Song, H. Su, J. Han, J. Xu and D. Zhang, *Sens. Actuators, B* 2010, **145**, 39-45.

66.   F. Song, H. Su, J. Han, D. Zhang and Z. Chen, *Nanotechnology*, 2009, **20**, 495502.

67.   Y. Chen, J. Gu, S. Zhu, T. Fan and Q. Guo, *Appl. Phys. Lett.* , 2009, **94**, 053901.

68.   Y. Chen, J. Gu, D. Zhang, S. Zhu, H. Su, X. Hu, C. Feng, W. Zhang, Q. Liu and A. R. Parker, *J. Mater. Chem.* , 2011, **21**, 15237-15237.

69.   W. Peng, X. Hu and D. Zhang, *J. Magn. Magn. Mater.* , 2011.

70.   W. Peng, S. Zhu, W. Wang, W. Zhang, J. Gu, X. Hu, D. Zhang and Z. Chen, *Adv. Funct. Mater.* , 2012, **22**, 2071.

71.   S. Zhu, X. Liu, Z. Chen, C. Liu, C. Feng, J. Gu, Q. Liu and D. Zhang, *J. Mater. Chem.* , 2010, **20**, 9126-9132.

72.   A. Saito, Y. Miyamura, M. Nakajima, Y. Ishikawa, K. Sogo, Y. Kuwahara and Y. Hirai, *J Vac Sci Technol B*, 2006, **24**, 3248-3251.

73.   A. Saito, M. Nakajima, Y. Miyamura, K. Sogo, Y. Ishikawa and Y. Hirai, *Nanoengineering: Fabrication, Properties, Optics, and Devices III*, 2006, **6327**, Z3270-Z3270.

74.   A. Saito, S. Yoshioka and S. Kinoshita, presented in part at the Proceedings of SPIE(Optical Systems Degradation, Contamination, and Stray Light: Effects, Measurements, and Control) 2004.

75.   Q. Zhao, T. Fan, J. Ding, D. Zhang, Q. Guo and M. Kamada, *Carbon*, 2010.

76.   J. Han, H. L. Su, F. Song, D. Zhang and Z. X. Chen, *Nanoscale*, 2010, **2**, 2203-2208.

77.   Y. Tan, X. Zang, J. Gu, D. Liu, S. Zhu, H. Su, C. Feng, Q. Liu, W. M. Lau, W.-J. Moon and D. Zhang, *Langmuir*, 2011, **27**, 11742–11746.

78.   Y. Tan, J. Gu, X. Zang, W. Xu, K. Shi, L. Xu and D. Zhang, *Angew. Chem. Int. Ed.* , 2011, **50**, 1-6.

79.   Y. W. Tan, J. J. Gu, L. H. Xu, X. N. Zang, D. Liu, W. Zhang, Q. L. Liu, S. M. Zhu, H. L. Su, C. L. Feng, G. L. Fan and D. Zhang, *Adv. Funct. Mater.* , 2012, **22**, 1578-1585.

80.   K. Watanabe, T. Hoshino, K. Kanda, Y. Haruyama, T. Kaito and S. Matsui, *J Vac Sci Technol B*, 2005, **23**, 570-574.

81.   K. Watanabe, T. Hoshino, K. Kanda, Y. Haruyama and S. Matsui, *Jpn J Appl Phys 2*, 2005, **44**, L48-L50.

82.   S. H. Kang, T. Y. Tai and T. H. Fang, *Curr. Appl Phys.* , 2010, **10**, 625-630.

83.   T. S. Kustandi, H. Y. Low, J. H. Teng, I. Rodriguez and R. Yin, *Small*, 2009, **5**, 574-578.

84.   R. Coath, 5, University of Southampton, 2007.

85.   Z. Xu, K. Yu, B. Li, R. Huang, P. Wu, H. Mao, N. Liao and Z. Zhu, *Nano Research*, 2011, **4**, 737-745.

86.   W. Zhang, D. Zhang, T. X. Fan, J. Ding, J. J. Gu, Q. Guo and H. Ogawa, *Mat Sci Eng C-Bio S*, 2009, **29**, 92-96.

87.   S. Zhu, D. Zhang, Z. Li, H. Furukawa and Z. Chen, *Langmuir*, 2008, **24**, 6292-6299.

88.   A. R. Maddocks and A. T. Harris, *Mater Lett*, 2009, **63**, 748-750.

89.   R. J. Martin-Palma, C. G. Pantano and A. Lakhtakia, *Appl. Phys. Lett.* , 2008, **93**, -.

90.   A. Lakhtakia, R. Martin-Palma, M. Motyka and C. Pantano, *Bioinspir. Biomim.*, 2009, **4**, 034001.

91.   T. Kawano, M. Sato, H. Yabu and M. Shimomura, *Biomater Sci-Uk*, 2014, **2**, 52-56.

92.   Y. Saito, M. Shimomura and H. Yabu, *Chem. Commun.* , 2013, **49**, 6081-6083.

93.   H. Yabu, R. Jia, Y. Matsuo, K. Ijiro, S.-a. Yamamoto, F. Nishino, T. Takaki, M. Kuwahara and M. Shimomura, *Adv. Mater.* , 2008, **20**, 4200-4204.

94.   H. Yabu, M. Takebayashi, M. Tanaka and M. Shimomura, *Langmuir*, 2005, **21**, 3235-3237.

95.   S. Chen, M.-H. Alves, M. Save and L. Billon, *Polymer Chemistry*, 2014.

96.   F. Galeotti, W. Mróz, G. Scavia and C. Botta, *Org. Electron.* , 2013, **14**, 212-218.

97.   A.-C. Courbaron Gilbert, C. Derail, N. E. El Bounia and L. Billon, *Polymer Chemistry*, 2012, **3**, 415-420.

98.   F. Galeotti, V. Calabrese, M. Cavazzini, S. Quici, C. Poleunis, S. Yunus and A. Bolognesi, *Chem. Mater.* , 2010, **22**, 2764-2769.

99.   C. Deleuze, M. H. Delville, V. Pellerin, C. Derail and L. Billon, *Macromolecules*, 2009, **42**, 5303-5309.

100.   L. Billon, M. Manguian, V. Pellerin, M. Joubert, O. Eterradossi and H. Garay, *Macromolecules*, 2008, **42**, 345-356.

101.   L. Ghannam, M. Manguian, J. Francois and L. Billon, *Soft Matter*, 2007, **3**, 1492-1499.

102.   X. Zang, Y. Ge, J. Gu, S. Zhu, H. Su, C. Feng, W. Zhang, Q. Liu and D. Zhang, *J. Mater. Chem.* , 2011, **21**, 13913-13919.

103.   B. Li, J. Zhou, R. Zong, M. Fu, Y. Bai, L. Li and Q. Li, *J. Am. Ceram. Soc.* , 2006, **89**, 2298-2300.

104.   T. Saison, C. Peroz, V. Chauveau, S. Berthier, E. Sondergard and H. Arribart, *Bioinspir. Biomim.*, 2008, **3**, -.

105.   M. Kolle, *Photonic structures inspired by nature*, Not Avail2010.

106.   C. Mille, E. C. Tyrode and R. W. Corkery, *Chem. Commun.* , 2011, **47**, 9873-9875.

107.   C. Mille, E. C. Tyrode and R. W. Corkery, *RSC Advances*, 2013, **3**, 3109-3117.

108.   A. G. Richards, *Ann. Entomol. Soc. Am.*, 1947, **40**, 227-240.

109.   J. D. Schiffman and C. L. Schauer, *Mat Sci Eng C-Bio S*, 2009, **29**, 1370-1374.

110.   R. Lakes, *Nature*, 1993, **361**, 511-515.

111.   Z. Mu, X. Zhao, Z. Xie, Y. Zhao, Q. Zhong, L. Bo and Z. Gu, *J. Mater. Chem. B*, 2013, **1**, 1607-1613.

112.   L. L. Hench and J. K. West, *Chem. Rev.* , 1990, **90**, 33-72.

113.   S. Mann, S. L. Burkett, S. A. Davis, C. E. Fowler, N. H. Mendelson, S. D. Sims, D. Walsh and N. T. Whilton, *Chem. Mater.* , 1997, **9**, 2300-2310.

114.   R. Withnall, J. Silver, T. G. Ireland, S. Zhang and G. R. Fern, *Optics and Laser Technology*, 2011, **43**, 401-409.

115.   J. Silver, T. Ireland and R. Withnall, *J Mater Res*, 2004, **19**, 1656-1661.

116.   J. Silver, R. Withnall, T. Ireland, G. Fern and S. Zhang, *Nanotechnology*, 2008, **19**, 095302.

117.   Y. Zheng, X. Gao and L. Jiang, *Soft Matter*, 2007, **3**, 178-182.

118.   M. Weatherspoon, 2008.

119.   F. Yao, Q. Q. Yang, C. Yin, S. M. Zhu, D. Zhang, W. J. Moon and Y. S. Kim, *Mater Lett*, 2012, **77**, 21-24.

120.   C. Yin, S. Zhu, Z. Chen, W. Zhang, J. Gu and D. Zhang, *J Mater Chem A*, 2013, **1**, 8367-8378.

121.   S. Lou, X. Guo, T. Fan and D. Zhang, *Energy Environ. Sci.* , 2012, **5**, 9195-9216.

122.   L. P. Biro, K. Kertesz, Z. Vertesy and Z. Balint, Photonic nanoarchitectures occurring in butterfly scales as selective gas/vapor sensors, 2008.

123.   L. Gonzalez-Urbina, K. Baert, B. Kolaric, J. Perez-Moreno and K. Clays, *Chem. Rev.* , 2012, **112**, 2268-2285.

124.   W. Zhang, J. Tian, Y. Wang, X. Fang, W. Chen, Q. Liu and D. Zhang, *J Mater Chem A*, 2014, **2**, 4543-4550.

125.   S. Mouchet, O. Deparis and J. P. Vigneron, Unexplained high sensitivity of the reflectance of porous natural photonic structures to the presence of gases and vapours in the atmosphere, 2012.

126.   F. Song, H. L. Su, J. J. Chen, D. Zhang and W. J. Moon, *Appl. Phys. Lett.* , 2011, **99**.

127.   B. Liu, W. Zhang, H. Lv, D. Zhang and X. Gong, *Mater Lett*, 2012, **74**, 43-45.

128.   L. J. Guo, *Adv. Mater.* , 2007, **19**, 495-513.

129. M. Sun, C. Luo, L. Xu, H. Ji, Q. Ouyang, D. Yu and Y. Chen, *Langmuir*, 2005, **21**, 8978-8981.
130. G. M. Zhang, J. Zhang, G. Y. Xie, Z. F. Liu and H. B. Shao, *Small,* 2006, **2**, 1440-1443.
131. X. N. Zang, Y. W. Tan, Z. Lv, J. J. Gu and D. Zhang, *Sens. Actuators, B* 2012, **166**, 824-828.
132. C. Marichy, M. Bechelany and N. Pinna, *Adv. Mater.* , 2012, **24**, 1017-1032.
133. M. Knez, K. Niesch and L. Niinisto, *Adv. Mater.* , 2007, **19**, 3425-3438.
134. S. M. George, *Chem. Rev.* , 2010 **110**, 111-131.
135. D. Gaillot, O. Deparis, V. Welch, B. Wagner, J. Vigneron and C. Summers, *Physical Review E*, 2008, **78**, 31922.
136. Y. Ding, S. Xu, Y. Zhang, A. C. Wang, M. H. Wang, Y. Xiu, C. P. Wong and Z. L. Wang, *Nanotechnology*, 2008, **19**, 355708.
137. O. Paris, I. Burgert and P. Fratzl, *MRS Bull.* , 2010, **35**, 219-225.
138. E. Iwase, K. Matsumoto and I. Shimoyama, *Proc Ieee Micr Elect*, 2004, 105-108.
139. M. Crne, V. Sharma, J. Blair, J. O. Park, C. J. Summers and M. Srinivasarao, *EPL (Europhysics Letters)*, 2011, **93**, 14001.
140. J. Christopher, D. Gaillot, C. Matija, J. Blair, O. Jung, M. Srinivasarao, O. Deparis, V. Welch and J. Vigneron, *J Nonlinear. Opt. Phys.*, 2010, **19**, 489-501.
141. G. Widawski, M. Rawiso and B. Francois, 1994.
142. T. Kawano, Y. Nakamichi, S. Fujinami, K. Nakajima, H. Yabu and M. Shimomura, *Biomacromolecules*, 2013, **14**, 1208-1213.
143. H. Yabu, K. Inoue and M. Shimomura, *Colloid Surface A*, 2006, **284**, 301-304.
144. S. I. Matsushita, N. Kurono, T. Sawadaishi and M. Shimomura, *Synthetic Met*, 2004, **147**, 237-240.
145. M. H. Stenzel-Rosenbaum, T. P. Davis, A. G. Fane and V. Chen, *Angew Chem Int Edit*, 2001, **40**, 3428-+.
146. C. X. Cheng, Y. Tian, Y. Q. Shi, R. P. Tang and F. Xi, *Langmuir*, 2005, **21**, 6576-6581.
147. N. Maruyama, T. Koito, J. Nishida, T. Sawadaishi, X. Cieren, K. Ijiro, O. Karthaus and M. Shimomura, *Thin Solid Films*, 1998, **327**, 854-856.
148. P. S. Shah, M. B. Sigman, C. A. Stowell, K. T. Lim, K. P. Johnston and B. A. Korgel, *Adv. Mater.* , 2003, **15**, 971-+.
149. H. M. Ma and J. C. Hao, *Chem-Eur J*, 2010, **16**, 655-660.
150. W. F. Bu, H. L. Li, H. Sun, S. Y. Yin and L. X. Wu, *J. Am. Chem. Soc.* , 2005, **127**, 8016-8017.
151. M. Tanaka, M. Takebayashi, M. Miyama, J. Nishida and M. Shimomura, *Bio-Med. Mater. Eng.* , 2004, **14**, 439-446.

152. A. E. Saunders, P. S. Shah, M. B. Sigman, T. Hanrath, H. S. Hwang, K. T. Lim, K. P. Johnston and B. A. Korgel, *Nano Lett.*, 2004, **4**, 1943-1948.
153. T. Nishikawa, J. Nishida, R. Ookura, S. I. Nishimura, S. Wada, T. Karino and M. Shimomura, *Mat Sci Eng C-Bio S*, 1999, **8-9**, 495-500.
154. M. Hernandez-Guerrero, E. Min, C. Barner-Kowollik, A. H. E. Muller and M. H. Stenzel, *J. Mater. Chem.*, 2008, **18**, 4718-4730.
155. B. de Boer, U. Stalmach, H. Nijland and G. Hadziioannou, *Adv. Mater.*, 2000, **12**, 1581-+.
156. H. Yabu and M. Shimomura, *Langmuir*, 2005, **21**, 1709-1711.
157. L. Li, Y. W. Zhong, C. Y. Ma, J. Li, C. K. Chen, A. J. Zhang, D. L. Tang, S. Y. Xie and Z. Ma, *Chem. Mater.*, 2009, **21**, 4977-4983.
158. Z. He, W. Zhang, W. Wang, M. Tassin, J. Gu, Q. Liu, S. Zhu, H. Su, C. Feng and D. Zhang, *J. Mater. Chem. B*, 2013, **1**, 1673-1677.
159. W. Wang, W. Zhang, J. Gu, Q. Liu, T. Deng, D. Zhang and H.-Q. Lin, *Sci. Rep-UK*, 2013, **3**.